International Journal of Advanced and Applied Sciences, 5(10) 2018, Pages: 106-114

Contents lists available at Science-Gate

International Journal of Advanced and Applied Sciences

Journal homepage: http://www.science-gate.com/IJAAS.html

Biomedical images enhancement based on swarm optimization and differential evolution technique

Abdullah Shawan Alotaibi *

Computer Science Department, Shaqra University, Shaqra, Saudi Arabia

ARTICLE INFO

Article history:
Received 10 May 2018
Received in revised form
14 August 2018
Accepted 26 August 2018

Keywords:
Matching pursuit
Differential evolution
Anisotropic atom
Genetic algorithm
Particle swarm optimization
Dynamic multi-swarm optimization

ABSTRACT

In this paper, we have introduced an effective technique to remove the noise in the MRI and CT medical images during the process of acquisition, transmission, storage or compression. Removing these noise from medical images must be done without affecting relevant features of the image. Many techniques, such as genetic algorithm, Particle Swarm Optimization, Dynamic Multi-Swarm Particle Swarm Optimization and matching pursuit algorithm are used for denoising MRI and CT images. These techniques need more time to remove noise from medical images and find local point optimal. The proposed Differential Evolution based on Matching Pursuit (DE-MP) is used to detect best atom dictionary. The initial dictionary is created from an anisotropic atom. To evaluate the performance of the proposed techniques, the results of the proposed algorithm were compared with the other algorithm. The numerical results show that the performance of the proposed algorithm is more efficient and faster than other algorithms for medical images denoising.

1. Introduction

Medical images play an essential role in analysis duties with applications in various knowledge domains, such as diagnoses illnesses and medicine. There are many problems facing medical specialists in the medical field such as: noise suppression and blurring. Although several image denoising techniques have been suggested in the literature, noise suppression in images still remains a challenging problem for researchers since the process of removing the noise from images can cause the removal of pertinent image features, such as edges and corners (Singh and Wadhwani, 2015). Therefore, one of the biggest problems is removing noise from images. Noise suppression can introduce artifacts or cause image blurring, which makes image denoising a complicated task. There are different methods have been proposed to remove noise from images; however, each one examines specific facts of the problem (Farouk et al., 2016).

Image denoising algorithms can be divided into three types: image denoising algorithm based on transform domain filtering, image denoising algorithm based on spatial filtering and image denoising based on learning. The denoising algorithm based on transform domain filtering includes wavelet transform, Fourier transform, Block-matching and 3D filtering (BM3D) algorithm, etc. (Geng et al., 2016, He et al., 2014). The second type is the denoising algorithm based on spatial filtering includes bilateral filtering, Gaussian filtering, guide filtering, nonlocal mean filtering, etc. (Geng et al., 2016, He et al., 2014). The third type is the denoising algorithm based on learning involves K- singular value decomposition (K-SVD) algorithm (He et al., 2014) large-scale sparse clustering (LSSC) algorithm (Liu et al., 2015) and clustering based sparse representation (CSR) algorithm (Yang et al., 2015). K-SVD is a dictionary learning algorithm. It is used to create a dictionary for a sparse representation (SR), via singular value decomposition (SVD) method. It works by iteratively alternating between sparse coding the input data based on the current dictionary, and updating the atoms in the dictionary to better fit the data. The K-SVD improved with different type of dictionary to form atoms of it such as: DCT (Elad and Aharon, 2006), Gabor Wavelet (Khedr et al., 2012), Log-Gabor (Wang et al., 2014) and Log Gabor Wavelet (Farouk et al., 2016). In Ruiz-Reyes et al. (2005), the space-alternating generalized expectation-maximization (SAGE) algorithm is used to estimate the values of parameter vector and minimum description length. In Wax and Ziskind (1989), the minimum description length (MDL) basic principle

* Corresponding Author.
Email Address: a.shawan@su.edu.sa
https://doi.org/10.21833/ijaas.2018.10.015

was incorporated in the algorithm to estimate the model order (i.e., the determination of the number of echoes). The matching pursuit (MP) is made by estimating and adding. MP algorithm has been applied for medical image denoising. The main problem of MP formula is to estimate the basic parameters of the original signal. First, MP matches a function to the original signal. Then, this function is subtracted from the signal to obtain the signal residue. In Toledo et al. (2013), GA algorithm is used to remove noise from the digital image and the numerical results proved that GA algorithm is better than traditional (state-of-the-art) denoising methods. In Davis (1991), GA based thresholding techniques are used in image denoising. It is used wavelet transform to remove Gaussian noise from medical images. GA algorithm finds the best threshold value and the level of decomposition for the Bayesian thresholding by the use of stochastic and randomized search algorithm compared with Visu shrink, sure shrink and Bayes shrink. The numerical results show that GA based thresholding techniques are better than Visu shrink, sure shrink and Bayes shrink. In Liu (2015), GA algorithm is used to derive the denoising results. In Korurek et al. (2010), GA algorithm is used to evaluate parameter values in a model for a near field effect of X-ray source. Also, GA-MP algorithm is used to reduce the computational cost of computing the projection of the signal. Genetic algorithm (GA) is still local optimization algorithm. So, it is applied to obtain the best solution does not give an optimal result and compromise between speed and accuracy, GA algorithm try to maximize this relation (Jansi and Subashini, 2013; Cui et al., 2014). Because of the randomness of the GA algorithm, the final solution will be suboptimal.

PSO algorithm is presented by Eberhart and Kennedy (1995). In Ashour et al. (2015), cuckoo search (CS) is used to find the optimal parameter settings for log transform and log transform is used in medical image enhancement algorithm. The numerical results proved that CS-log transform is faster than PSO algorithm. In Jansi and Subashini (2013), PSO is used to find the optimal value of the regularization parameter of total variation method that helps total variation method to remove noise in magnetic resonance imaging (MRI) images. In Hu et al. (2015), PSO is used to find the optimal weighted factor that was inserted into weighted sub wavelets then classical Shearlet transform is used to decompose noised image into these sub wavelets under multiscale and multi-orientation. PSO is simple algorithm but it has been slow so that, PSO improved with MP algorithm to find the best atom searching problem (Liang and Suganthan, 2006).

DMS-PSO algorithm is appeared to avoid the disadvantages of PSO algorithm. In the DMS-PSO, the population is divided into several small groups. In Chen et al. (2013), the DMS-PSO-MP was developed by Discrete Coefficient Mutation (DCM) strategy to improve the local searching ability of DMS-PSO in the MP approach over the anisotropic atom dictionary. Experimental results show that DMS-PSO with DCM strategy is better than other popular versions of PSO.

This paper aims to combine DE and MP algorithms for denoising medical images, the anisotropic atom is used to generate over-complete dictionary and DE is applied to detect best atom of dictionary based on MP algorithm. Generally speaking, each algorithm has some filtering and threshold parameters. Taking variety kinds of images into account, it is a key problem of how to set these parameters in denoising algorithms under different conditions to achieve better performance and short execution. The values of the parameter vector and optimal model can be estimated by merging DE algorithm with MP algorithm. The rest of this paper is organized as follows: Section 2 sparse representation of images, matching pursuit of images and differential evolution algorithm are discussed. Section 3 the proposed algorithm DE-MP is discussed. The numerical results of DE algorithm in image denoising is discussed and compared with other methods in section 4. Finally, conclusions are shown in Section 5.

2. Sparse representation of images

Sparse representation of images is used to generate a set of atoms $d_i \in R^m$ that form the dictionary $D \in R^{m \times k}$ and it is defined mathematical equation as:

$$y_i = Dx_i \tag{1}$$

Eq. 1 can be rewritten as Eq. 2:

$$\min_{D,x} ||y - Dx||_2 \quad s.t \quad ||x||_0 < l. \tag{2}$$

where $||.||_0$ is the L_0 semi-norm, which counting the non-zero entries of a vector, $||.||_2$ is the L_0 - norm, which represents the Euclidean length of a vector. l is a threshold that control the sparseness of the vector x. The over-complete dictionary D is generated by anisotropic atom. DE algorithm is used to select the best atom from the dictionary and matching pursuit algorithm (MP) is used to find sparse representation X_i of y_i.

2.1. Matching pursuit of images

MP is a greedy algorithm that is used to utilize signal decomposition based on a redundant dictionary called the over-complete dictionary with each element called an atom (Davis, 1991). Best atom can be selected from atoms of the dictionary when MP applied. MP depends on over-complete dictionary, in each iteration, the best matching atom can be available in over-complete dictionary (Hu et al., 2015).

Let $D = \{g_\gamma\}_{\gamma\in\Gamma}$ is the atoms of the dictionary, for arbitrary image of size $\times c$, Γ is the set of all indexes γ and $||g_\gamma|| = 1$ (Jansi and Subasini, 2013). Let y is an arbitrary signal. The initial step of a Matching

Pursuit is always to approximate y by the projecting it on a vector $g_{\gamma_0} \in D$

$$y = < y, g_{\gamma_0} > g_{\gamma_0} + R_y \quad (3)$$

where $< y, g_{\gamma_0} > g_{\gamma_0}$ is projection of y onto atom g_{γ_0} and R_y is the residual of the original signal. Since the residual R_y is orthogonal to g_{γ_0} (Liang and Suganthan, 2006).

$$||y||^2 = | < y, g_{\gamma_0} > |^2 \, ||g_{\gamma_0}||^2 + ||R_y||^2 \quad (4)$$
$$||y||^2 = | < y, g_{\gamma_0} > |^2 + ||R_y||^2, \ where \ ||g_{\gamma_0}||^2 = 1 \quad (5)$$

where $||g_{\gamma_0}||^2 = 1$. In term $||R_y||^2 = \ ||y||^2 - | < y, g_{\gamma_0} > |^2$ must be minimized, so $g_{\gamma_0} \in D$ must be chosen to maximize$| < y, g_{\gamma_0} > |$. After N iterations, the original signal can be reconstructed via the selected atom g_{γ_n}:

$$y \approx \sum_{n=0}^{N-1} < R_y^n, g_{\gamma_n} > g_{\gamma_n} \quad (6)$$

The process of generating the g_γ is the one of the main steps in denoising processes. So, the Gaussian function is used as in Eq. 7. The essential function is a Gaussian in one axis and the second derivative of the Gaussian in the various other axis (Liang and Suganthan, 2006).

$$g_\gamma = (2 - 4h^2)e^{-\frac{1}{4}(h^2+w^2)}. \quad (7)$$

Eq. 7 is used to generate the dictionary with translation, rotation, translation and scaling factor in x and y directions, i.e., θ, u, v, s_x, s_y respectively. Anisotropic atom was used to find h, w.

$$h = \left(\cos(\theta) \ * h_x + \sin(\theta) * h_y\right)/2^{\left(\frac{stx}{NN}\right)} \quad (8)$$
$$w = \left(\cos(\theta) * h_y - \sin(\theta) * h_x\right)/2^{\left(\frac{sty}{NN}\right)} \quad (9)$$

where $h_x, h_y, \theta, stx \ and \ sty$ are translations in x, y directions, rotation angel, arbitrary columns of the population respectively, $NN = 5$.

2.2. Differential evolution algorithm

In Storn and Price (1997) DE algorithm developed by Storn and Price. It really is inspired by natural selection and natural genetics. The main difference between DE and GA algorithms is that GA algorithm based on the crossover (recombination) while DE algorithm based on mutation operation. DE algorithm is same as genetic algorithms (i.e., DE algorithm have the same steps of GA algorithm).

The DE algorithm is heuristic algorithm that has three advantages; finding the best global minimum of a multi-modal search space regardless the values of the initial parameter, it using a little number of control parameters and its convergence faster than GA, PSO and DMS-PSO algorithms (Karaboga and Cetinkaya, 2004). Fig. 1 shows the main steps of DE algorithm. In the DE algorithm, the solution has the form:

$$Y_{i,G} = [Y1_{i,G}, Y2_{i,G}, Y3_{i,G}, \ldots, Yn_{i,G}], \quad i = 1,2,3, \ldots, N.$$

where N, n are the size of population P and number of parameters respectively The DE algorithm can be presented as the following steps. The first step of DE algorithm is called initialization, lower (L) and upper (U) bound of each solution are defined and then randomly generate initial populations P and should cover all entire solutions (i.e. θ, u, v, s_x, s_y) (Bhandari et al., 2016).

$$Y_i^L \le Y1_{i,G} \le Y_i^U. \quad (10)$$

Then the fitness function is measured. Then, randomly select three solutions $Y1_{i,G}, Y2_{i,G} \ and \ Y3_{i,G}$ from population P (mutation step). DE algorithm generates new vector called donor vector by adding the weight difference of two of the vectors to the third as equation

$$v_{i,G+1} = Y1_{i,G} + F(Y2_{i,G} - Y3_{i,G}) \quad (11)$$

where the mutation factor F is constant $\in$ [0, 2], $v_{i,G+1}$ is called the donor vector. The next step is called crossover (recombination). Here, new vector called trial vector $u_{i,G+1}$ is developed from the elements of both target vector $Y_{i,G}$ and donor vector $v_{i,G+1}$. Elements of the donor vector enter the trial vector with probability Crossover Rate (CR).

$$u_{i,G+1} = \begin{cases} v_{j,i,G+1} \ \ if \ rand_{i,j} \le CR \ \ or \ j = i_{rand} \\ Y_{j,i,G} \ \ \ if \ rand_{i,j} > CR \ or \ j \ne i_{rand} \end{cases}. \quad (12)$$

CR is constant $\in$ [0, 1]. Where $i = 1,2, \ldots, N; j = 1,2, \ldots, n \ and \ i_{rand}$ is a random integer from [1, 2, 3…n]. The final step of DE algorithm called Selection step. Which a new vector called trail vector is created. The target vector $Y_{i,G}$ is compared with the trial vector $u_{i,G+1}$ and the one with the lowest function value is admitted to the next generation.

$$Y_{i,G+1} = \begin{cases} u_{i,G+1} \ \ if \ \ f(u_{i,G+1}) \le f(X_{i,G}) \\ \ \ Y_{i,G} \qquad\qquad otherwise \end{cases} \quad (13)$$

3. The proposed algorithm

In this section the proposed algorithm is introduced (i.e., Denoising image based on DE-MP algorithm). It can be presented as the following: Noisy image y and error tolerance are considered inputs to the proposed algorithm. Anisotropic atom is used Eq. 7 to form the over complete dictionary. The vector which is defined as $g_{\gamma_{i,0}}, g_{\gamma_{i,1}}, g_{\gamma_{i,2}}, \ldots, g_{\gamma_{i,n-1}} \in D$ could be gotten $g_{\gamma_i} = (g_{\gamma_{i,0}}, g_{\gamma_{i,1}}, g_{\gamma_{i,2}}, \ldots, g_{\gamma_{i,n-1}})$ then randomly initialized the population of $n \ and \ Dim \ = \ 300$ to be represented in one column of over complete dictionary D. The problem $y \ = \ Dx \ + \ \varepsilon$ must be solved where sparse representation x of image y can be defined as $x = (x_1, x_2, x_3, \dots, x_n)^T$.

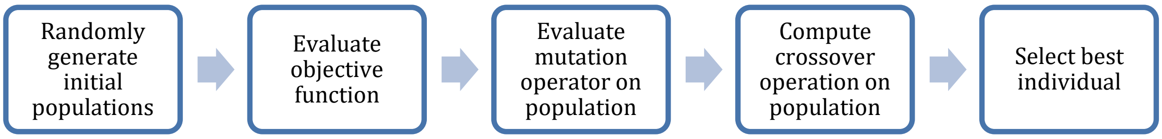

Fig. 1: Shows the main steps of DE algorithm

The previous problem can be solved as $\min_{D,x} ||y - Dx||_2 \ s.t \ ||x|| < \varepsilon, \varepsilon \in \mathrm{R}$ If the error tolerance $\varepsilon <= 0.01$ now, the image is really cleaned. Then, compute the performance of clean image. If this condition is not satisfied (i.e., $\varepsilon <= 0.01$) then, use Eq. 11 to find mutation operators on populations. The donor vector and target vector are used to find trial vector in crossover step. Use Eq. 13 to select best atom of over complete dictionary. Then, use MP algorithm to find sparse representation x of image y and then go to solve the previous problem. Simply DE-MP denoising algorithm can be presented in Fig. 2. The denoised image based on DE-MP can be given as following steps:

DE-MP denoising algorithm

Input: *noisy image and initialize error tolerance ε.*
Step 1: generate atoms of dictionary (use Eq. 5).
Step 2: construct a random initial population of n and dimension (Dim=300).
Step 3: $for\ i = 1{:}n$
evaluate fitness function
if $\varepsilon \leq 0.01$ *then*
Output: *clean image.*
Else
Step 4: evaluate mutation operators on populations (use Eq. 10).
Step 5: Find crossover operators on populations (use Eq. 11).
Step 6: select best atom (use Eq. 12).
Step 7: use MP to find sparse representation of image.
Step 8: go to step 3, to calculate fitness function.

4. Numerical results

This section reports and discusses the experimental results obtained with the proposed algorithm (DE-MP) for medical images denoising. The method was tested in several images; five of them were selected to illustrate the results. These images present dimensions of 128 × 128, 64 × 64, 128 × 128, 64 × 64, 128 × 128, and 64 × 64 pixels, respectively Farouk et al. (2016), and they were corrupted with additive Gaussian noise $N(0, \sigma^2)$, where σ^2 is the estimated noise deviation with noise levels $\sigma = 10, 20, 30, 40, 50, 60, 70, 80$ and 90. The first image (MRI image) was used with different resolution 128×128 and 64×64.

All experiments are performed on a PC running MATLAB(R) R2012b 64-bit in Windows(R) 10 with 4 GB RAM and Intel(R) CORE(R) i5 M-430 processor is used to conduct the whole experiment. In this paper, the performance is measured by using two methods shown as the following:

- **Peak Signal to Noise Ratio (PSNR):** The Peak Signal to Noise Ratio (PSNR) is used to measure the performance and it is defined as (Chen et al., 2013):

$$PSNR = 20\ log_{10}(\frac{MAX_{y_0}}{\sqrt{MSE}}), \tag{14}$$

the performance was measured at different noise levels. Where the MSE (Mean Squared Error) is:

$$MSE = \frac{1}{mn}\sum_{i=0}^{m-1}\sum_{j=0}^{n-1}||y_0(i,j) - y(i,j)||^2, \tag{15}$$

where y_0 and y are the original and denoised images respectively. m is represents the numbers of rows of pixels of the images y_0 and y. n is represents the number of columns of pixels of the images y_0 and y.

- **Structural Similarity Index (SSIM):** The Structural Similarity Index (SSIM) is used to measure image quality. SSIM is based on the computation of three terms, the luminance term (l), the contrast term(c), and the structural term (s) (Farouk et al., 2016). The overall index is a multiplicative combination of the three terms.

$$SSIM(p_1, p_2) = [l(p_1, p_2)]^{\lambda}.[c(p_1, p_2)]^{\beta}.[s(p_1, p_2)]^{\nu} \tag{16}$$

where:

$$l(p_1, p_2) = \frac{2\mu_{p1}\mu_{p2} + c_1}{\mu_{p1}^2 + \mu_{p2}^2 + c_1} \tag{17}$$

$$c(p_1, p_2) = \frac{2\sigma_{p1}\sigma_{p2} + c_2}{\sigma_{p1}^2 + \sigma_{p2}^2 + c_2} \tag{18}$$

$$s(p_1, p_2) = \frac{\sigma_{p1p2} + c_3}{\sigma_{p1}\sigma_{p2} + c_3}, \tag{19}$$

where $\mu_{p1}, \mu_{p2}, \sigma_{p1}, \sigma_{p2}$ and σ_{p1p2} are the local means, standard deviations, and cross-covariance for images p_1, p_2. If $\lambda = \beta = \nu = 1$ (the default for Exponents), and $c_3 = \frac{c_2}{2}$ (default selection of c_3) the index simplifies to:

$$SSIM(p_1, p_2) = \frac{(2\mu_{p1}\mu_{p2} + c_1)(2\sigma_{p1p2} + c_2)}{(\mu_{p1}^2 + \mu_{p2}^2 + c_1)(\sigma_{p1}^2 + \sigma_{p2}^2 + c_2)} \tag{20}$$

For DMS-MP Regroup Period is 3 and 5 groups are formed with each group's population size is 60. Population size is randomly in GA-MP. The population size of proposed algorithm is N=60 and a number of parametersN=60. In DMS-PSO and standard PSO, the Linear Decreasing Weight (LDW) (Farouk et al., 2016) is used. In LDW, weight is updated as generation and it can be computed using the following formula:

$$W_G = W_{min} + (W_{max} - W_{min}) \times \frac{G_{max} - G}{G_{max}}, \quad (21)$$

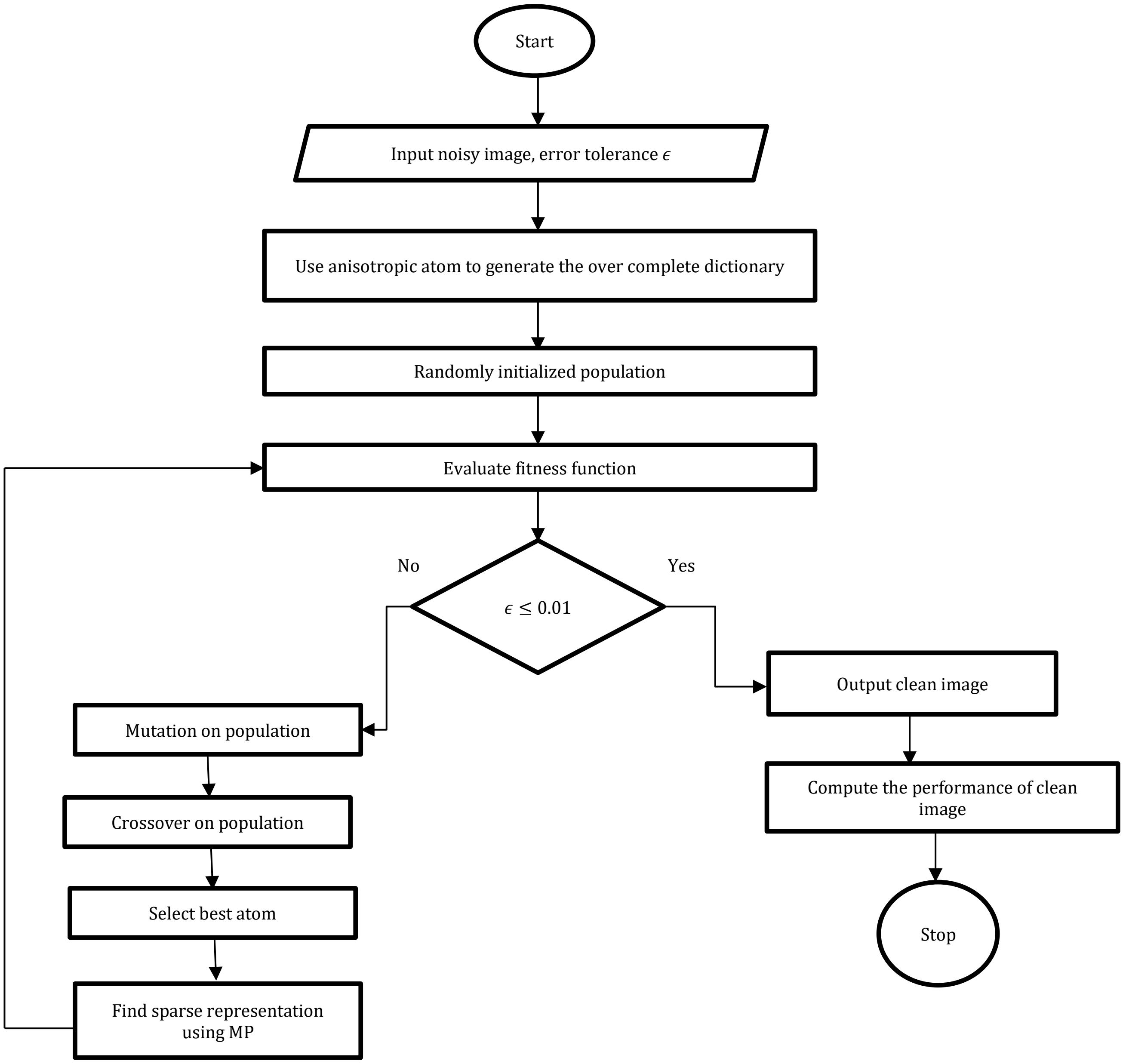

Fig. 2: Algorithm flowchart of MP optimized by improved DE

where G_{max} shows maximum generation. In this paper, W_{max} and W_{min} are set to 0.9, 0.2 respectively. In Table 1 and Table 2, the PSO-MP, DMS-PSOMP, GA-MP and the proposed algorithm have been developed using anisotropic atom. The MP algorithm improved with DMS-PSO, PSO, GA and DE algorithm, in which the best results are highlighted (in bold red). In Table 3, it is clear that proposed algorithm which improved with anisotropic atom is better and faster than PSO, DMS-PSO and GA algorithms. The numerical results indicated that several final solutions (images) can be returned by the proposed method within a short execution. In case 128 × 128 and 64 × 64, the average performance was calculated for each algorithm. PSNR of proposed algorithm, Standard-PSO, DMS-PSO and GA are shown. The average performance is converged for each medical image. It's clear that proposed algorithm outperforms the others with a PSNR of proposed algorithm; Standard-PSO, DMS-PSO and GA are shown. The average performance is converged for each medical image. It's clear that proposed algorithm outperforms the others with a PSNR of 25.54 dB, 23.57 dB, 23.13 dB, 21.17 dB, 23.13 dB and 20.44 dB with image resolution 128 × 128, 64 × 64, 128 × 128, 64 × 64, 128 × 128 and 64 × 64 respectively. PSNR boosts an increase from 21.57 dB to 30.73 dB, 20.34 dB to 27.20 dB, 19.99 dB to 26.89 dB, 18.97 dB to 23.46 dB, 20.51 dB to 26.26 dB and 18.34 dB to 22.67 dB with image resolution 128× 128, 64× 64, 128× 128, 64× 64, 128 × 128 and 64 × 64 respectively.. Obvious lower execution of the proposed algorithm can be seen in Fig. 3-8. The average time comparison of different algorithms with image resolution 128 × 128 and 64 × 64 is shown in Fig. 9, it is clear that the proposed algorithm takes shorter execution time than other algorithms.

In Table 2, the SSIM is used to measure the performance of medical images. The best results are highlighted (in bold red). It is clear that proposed algorithm which improved with anisotropic atom is better than PSO, DMS-PSO and GA algorithms. Table 3 shows that execution time of DMS-PSO, Standard PSO, GA-MP and the proposed algorithm that developed by anisotropic atom with different values of sigma $\sigma = 10, 30, 50, 70,$ and 90. The best results are highlighted (in bold red). It is clear that proposed algorithm is faster than other algorithms.

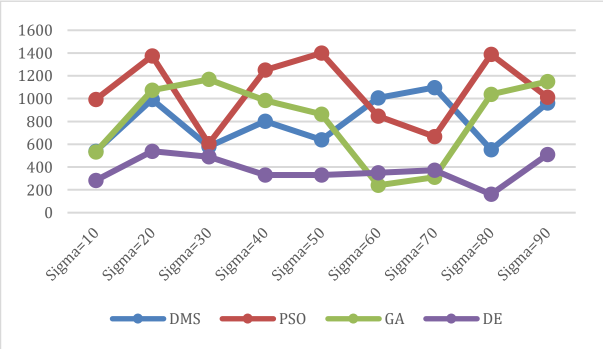

Fig. 3: Total time comparison of different algorithms with MRI image resolution 128 × 128

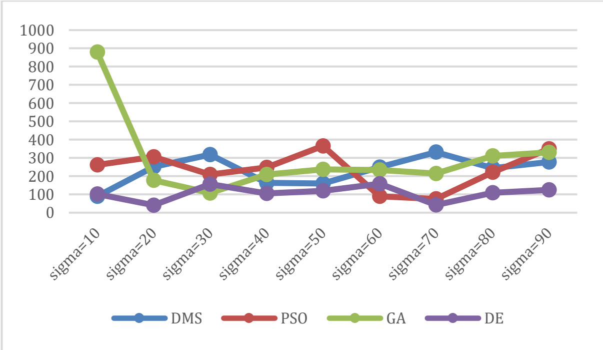

Fig. 4: Total time comparison of different algorithms with MRI image resolution 64 × 64

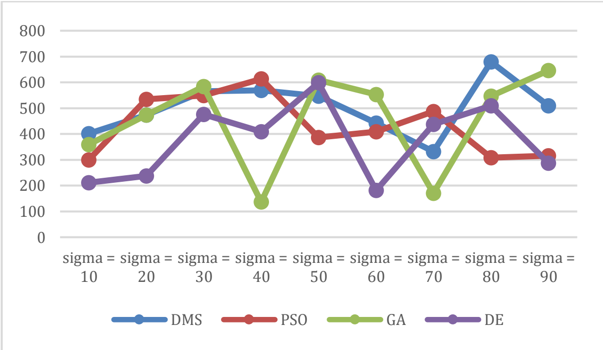

Fig. 5: Total time comparison of different algorithms with second image

Table 1: Comparison between the DMS-PSO, Standard PSO, GA-MP and the proposed algorithm that developed by anisotropic atom with different values of sigma

Sigma	SSIM Algorithms				
	Size of MRI image	DMS-PSO-MP	stand-PSO-MP	GA-MP	DE-MP
Sigma=10	128x128	0.81	0.82	0.83	0.83
	64x64	0.75	0.76	0.76	0.77
	128x128	0.84	0.83	0.79	0.83
	64x64	0.76	0.77	0.70	0.77
	128x128	0.85	0.84	0.85	0.84
	64x64	0.83	0.82	0.83	0.8
Sigma=30	128x128	0.52	0.54	0.52	0.54
	64x64	0.54	0.55	0.54	0.54
	128x128	0.71	0.65	0.68	0.67
	64x64	0.59	0.60	0.60	0.63
	128x128	0.59	0.58	0.59	0.68
	64x64	0.70	0.70	0.68	0.71
Sigma=50	128x128	0.36	0.38	0.37	0.38
	64x64	0.39	0.43	0.39	0.43
	128x128	0.52	0.53	0.50	0.52
	64x64	0.48	0.48	0.45	0.50
	128x128	0.44	0.44	0.43	0.42
	64x64	0.60	0.60	0.60	0.60
Sigma=70	128x128	0.28	0.29	0.29	0.30
	64x64	0.31	0.34	0.32	0.33
	128x128	0.43	0.48	0.41	0.44
	64x64	0.41	0.38	0.40	0.40
	128x128	0.34	0.34	0.35	0.36
	64x64	0.54	0.52	0.55	0.54
Sigma=90	128x128	0.49	0.51	0.52	0.50
	64x64	0.20	0.24	0.22	0.24
	128x128	0.24	0.28	0.25	0.26
	64x64	0.37	0.38	0.38	0.39
	128x128	0.35	0.35	0.35	0.35
	64x64	0.29	0.30	0.28	0.32
Average	128x128	0.49	0.51	0.51	0.51
	64x64	0.44	0.46	0.45	0.46
	128x128	0.55	0.55	0.53	0.54
	64x64	0.52	0.52	0.51	0.54
	128x128	0.51	0.51	0.51	0.53
	64x64	0.59	0.59	0.59	0.61

Table 2: Shows that Comparison between the DMS-PSO, Standard PSO, GA-MP and the proposed algorithm that developed by anisotropic atom with different values of sigma $\sigma = 10, 30, 50, 70$ and 90

Sigma	PSNR Algorithms				
	Size of MRI image	DMS-PSO-MP	stand-PSO-MP	GA-MP	DE-MP
Sigma=10	128x128	30.75	30.69	30.75	30.73
	64x64	27.21	27.26	27.25	27.20
	128x128	26.50	26.48	26.54	26.89
	64x64	23.32	23.22	23.33	23.46
	128x128	26.17	26.20	26.21	26.26
	64x64	22.38	22.23	22.38	22.67
Sigma=30	128x128	27.57	27.58	27.57	27.54
	64x64	25.49	25.27	25.18	25.24
	128x128	24.59	24.52	24.60	24.64
	64x64	22.21	22.42	22.38	22.71
	128x128	24.53	24.76	24.49	24.67
	64x64	21.48	21.47	21.45	21.90
Sigma=50	128x128	24.97	25.26	25.05	25.26
	64x64	23.21	23.39	23.18	23.37
	128x128	22.78	22.62	22.68	22.53
	64x64	21.08	21.07	21.03	21.35
	128x128	22.87	22.91	22.82	22.90
	64x64	20.10	20.29	18.55	20.31
Sigma=70	128x128	23.20	22.95	22.82	23.20
	64x64	21.64	21.35	21.55	21.81
	128x128	21.26	21.18	21.15	21.22
	64x64	19.92	19.36	19.90	19.63
	128x128	21.45	21.37	21.42	21.60
	64x64	19.11	19.29	18.16	19.13
Sigma=90	128x128	21.19	21.12	21.11	21.57
	64x64	20.18	20.27	20.37	20.34
	128x128	19.96	19.88	19.88	19.99
	64x64	18.51	18.37	18.64	18.97
	128x128	20.26	20.13	20.42	20.51
	64x64	17.88	18.03	17.89	18.34
Average	128x128	25.54	25.52	25.46	25.66
	64x64	23.55	23.51	23.51	23.59
	128x128	23.02	22.94	22.94	23.05
	64x64	21.0	20.89	21.06	21.22
	128x128	23.07	23.08	23.07	23.19
	64x64	20.20	20.26	19.69	20.47

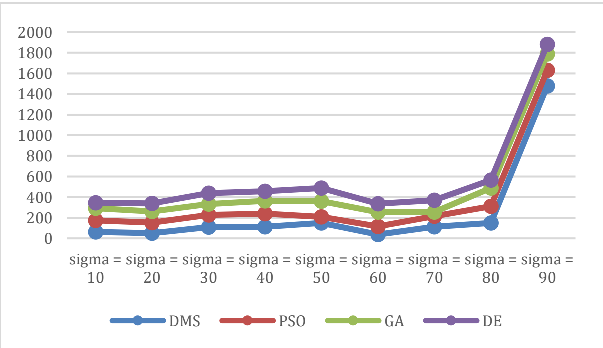

Fig. 6: Total time comparison of different algorithms with third image resolution 64 × 64

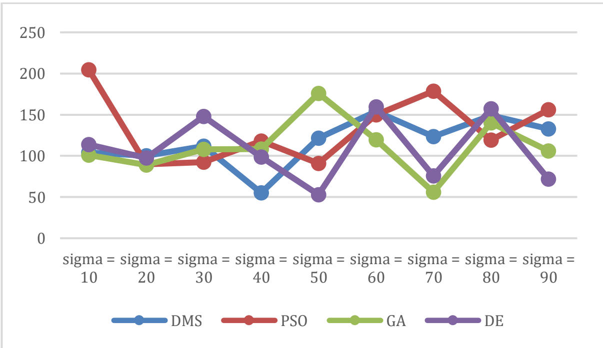

Fig. 8: Total time comparison of different algorithms with fifth image resolution 64 × 64

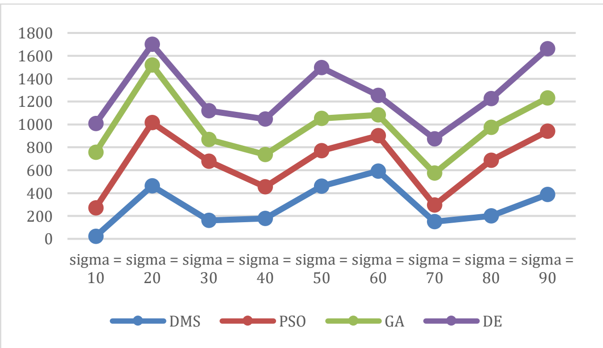

Fig. 7: Total time comparison of different algorithms with fourth image

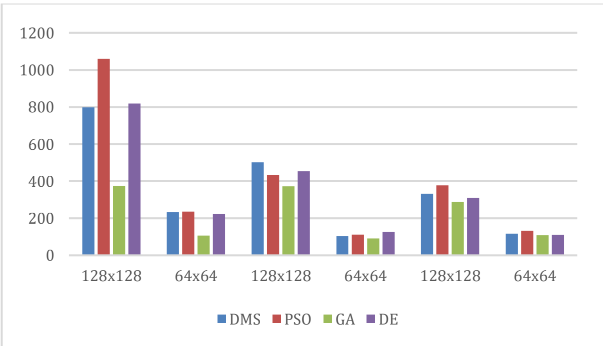

Fig. 9: Average time comparison of different algorithms with image resolution 128 × 128 and 64 × 64

Table 3: Comparison between execution time of the DMS-PSO, Standard PSO, GA-MP and the proposed algorithm that developed by anisotropic atom with different values of sigma

Sigma	TIME Algorithms				
	Size of MRI image	Time of DMS-PSO-MP	Time of stand-PSO-MP	Time of GA-MP	Time of DE-MP
Sigma=10	128x128	538.93	993.63	531.31	283.61
	64x64	89.56	261.91	88.04	102.07
	128x128	401.44	300.11	359.25	211.67
	64x64	63.71	111.75	115.52	55.14
	128x128	22.38	248.57	485.20	250.29
	64x64	103.88	204.48	100.77	113.67
Sigma=30	128x128	580.21	604.28	1168.6	491.32
	64x64	318.50	209.86	108.22	156.74
	128x128	565.61	549.32	584.17	475.96
	64x64	109.77	117.11	105.8	104.44
	128x128	160.14	516.69	190.46	253.22
	64x64	111.74	92.34	107.95	147.95
Sigma=50	128x128	640.44	1400.1	863.02	331.02
	64x64	160.60	356.68	237.96	120.10
	128x128	546.7	385.97	608.57	598.19
	64x64	150.09	57.67	152.48	128.41
	128x128	459.78	311.44	280.63	445.65
	64x64	121.63	90.76	157.80	52.89
Sigma=70	128x128	1098	668.37	311.25	372.96
	64x64	331.3	75.34	214.84	43.08
	128x128	331.97	487.08	170.18	437.17
	64x64	113.45	101.63	41.31	113.75
	128x128	150.62	143.95	279.23	301.97
	64x64	123.44	178.46	55.98	75.68
Sigma=90	128x128	963.43	1013.4	1150.8	508.89
	64x64	277.82	350.28	329.49	125.65
	128x128	508.81	315.23	645.91	286.77
	64x64	147.9	150.42	160.11	91.79
	128x128	387.51	552.80	290.50	430.11
	64x64	132.71	155.89	105.93	71.83
Average	128x128	797.67	1060.4	818.08	374.24
	64x64	231.92	235.43	222.13	106.93
	128x128	501.95	433.61	453.16	371.77
	64x64	103.94	111.66	124.87	91.99
	128x128	332.83	377.63	309.37	287.95
	64x64	116.85	133.24	109.50	108.32

5. Conclusion

This paper presented image denoising method using a Differential Evolution algorithm to suppress noise from medical images. A representation of populations is proposed based on the pixel matrix in such way that tailor-made crossover and mutation operators are designed. Preliminary experiments conducted on a set of medical images indicate the proposed algorithm, producing superior results compared to PSO-MP, DMS-PSO-MP and GA-MP denoising methods. The reported computational results indicated that several final solutions (images) can be returned by the proposed method within a short execution. The image quality that obtained by the proposed algorithm increases along increase in population size. The solution quality measured using PSNR and SSIM for these final solutions. In fact, the proposed method was able to outperform some of these methods in all results, taking into account the average and the best solutions found.

References

Ashour AS, Samanta S, Dey N, Kausar N, Abdessalemkaraa WB, and Hassanien AE (2015). Computed tomography image enhancement using cuckoo search: a log transform based approach. Journal of Signal and Information Processing, 6(3): 244-251.

Bhandari AK, Kumar D, Kumar A, and Singh GK (2016). Optimal sub-band adaptive thresholding based edge preserved satellite image denoising using adaptive differential evolution algorithm. Neurocomputing, 174: 698-721.

Chen C, Liang JJ, Qu BY, and Niu B (2013). Using dynamic multi-swarm particle swarm optimizer to improve the image sparse decomposition based on matching pursuit. In the International Conference on Intelligent Computing, Springer, Berlin, Heidelberg: 587-595.

Cui L, Wu N, Wang W, and Kang C (2014). Sensor-based vibration signal feature extraction using an improved composite dictionary matching pursuit algorithm. Sensors, 14(9): 16715-16739.

Davis L (1991). Handbook of genetic algorithms. Van Nostrand Reinhold, New York, USA.

Eberhart R and Kennedy J (1995). A new optimizer using particle swarm theory. In the 6th International Symposium on Micro Machine and Human Science, IEEE, Nagoya, Japan: 39-43.

Elad M and Aharon M (2006). Image denoising via sparse and redundant representations over learned dictionaries. IEEE Transactions on Image processing, 15(12): 3736-3745.

Farouk RM, Elsayed M, and Aly M (2016). Medical image denoising based on log-gabor wavelet dictionary and K-SVD algorithm. International Journal of Computer Applications, 141(1): 27-32.

Geng Y, Chen J, Fu R, Bao G, and Pahlavan K (2016). Enlighten wearable physiological monitoring systems: On-body RF characteristics based human motion classification using a support vector machine. IEEE Transactions on Mobile Computing, 15(3): 656-671.

He J, Geng Y, Liu F, and Xu C (2014). CC-KF: Enhanced TOA performance in multipath and NLOS indoor extreme environment. IEEE Sensors Journal, 14(11): 3766-3774.

Hu K, Song A, Xia M, Fan Z, Chen X, Zhang R, and Zheng Z (2015). An image filter based on shearlet transformation and particle swarm optimization algorithm. Mathematical Problems in Engineering, 2015: Article ID 414561, 9 pages. https://doi.org/10.1155/2015/414561

Jansi S and Subashini P (2013). Particle swarm optimization based total variation filter for image denoising. Journal of Theoretical and Applied Information Technology, 57(2): 169-173.

Karaboga N and Cetinkaya B (2004). Performance comparison of genetic and differential evolution algorithms for digital FIR filter design. In the International Conference on Advances in Information Systems, Springer, Berlin, Germany: 482-488.

Khedr W, Ali R, and Ismail F (2012). Image denoising using K-SVD algorithm based on Gabor wavelet dictionary. International Journal of Computer Applications, 59(2): 30-33.

Korurek M, Yüksel A, Iscan Z, Dokur Z, and Ölmez T (2010). Retrospective correction of near field effect of X-ray source in radiographic images by using genetic algorithms. Expert Systems with Applications, 37(3): 1946-1954.

Liang JJ and Suganthan PN (2006). Dynamic multi-swarm particle swarm optimizer with a novel constraint-handling mechanism. In the IEEE Congress on Evolutionary Computation, IEEE, Vancouver, Canada: 9-16.

Liu G, Geng Y, and Pahlavan K (2015). Effects of calibration RFID tags on performance of inertial navigation in indoor environment. In the International Conference on Computing, Networking and Communications, IEEE, Garden Grove, USA: 945-949.

Liu Y (2015). Image denoising method based on threshold, wavelet transform and genetic algorithm. International Journal of Signal Processing, Image Processing and Pattern Recognition, 8(2): 29-40.

Ruiz-Reyes N, Vera-Candeas P, Curpian-Alonso J, Mata-Campos R, and Cuevas-Martinez JC (2005). New matching pursuit-based algorithm for SNR improvement in ultrasonic NDT. NDT and E International, 38(6): 453-458.

Singh S and Wadhwani S (2015). Genetic algorithm based medical image denoising through sub band adaptive thresholding. International Journal of Science, Engineering and Technology Research (IJSETR), 4(5): 1481-1485.

Storn R and Price K (1997). Differential evolution–a simple and efficient heuristic for global optimization over continuous spaces. Journal of Global Optimization, 11(4): 341-359.

Toledo CF, de Oliveira L, da Silva RD, and Pedrini H (2013). Image denoising based on genetic algorithm. In the IEEE Congress on Evolutionary Computation, IEEE, Cancun, Mexico: 1294-1301.

Wang B, Ding D, Yang J, and Kong B (2014). An optimization sparse representation algorithm based on Log Gabor. International Journal of Image Processing, Image Processing and Pattern Recognition, 7(4): 221-230.

Wax M and Ziskind I (1989). Detection of the number of coherent signals by the MDL principle. IEEE Transactions on Acoustics, Speech, and Signal Processing, 37(8): 1190-1196.

Yang J, Chen B, Zhou J, and Lv Z (2015). A low-power and portable biomedical device for respiratory monitoring with a stable power source. Sensors, 15(8): 19618-19632.